AGU PUBLICATIONS

Geophysical Research Letters

RESEARCH LETTER
10.1002/2017GL076606

**Key Points:**
- Existing studies of the DWH assumed bubbly flow in the well riser; we showed that the flow might have been churn, where oil and gas tumble within the pipe
- Churn flow results in much larger energy dissipation, and if presented and neglected, could cause one to overestimate the oil discharge
- Churn flow results in a smaller oil droplet size distribution and could impact applied dispersant effectiveness

**Supporting Information:**
- Supporting Information S1
- Movie S1
- Movie S2
- Movie S3

**Correspondence to:**
M. C. Boufadel,
boufadel@gmail.com

**Citation:**
Boufadel, M. C., Gao, F., Zhao, L., Özgökmen, T., Miller, R., King, T., et al. (2018). Was the Deepwater Horizon well discharge churn flow? Implications on the estimation of the oil discharge and droplet size distribution. *Geophysical Research Letters*, *45*. https://doi.org/10.1002/2017GL076606

Received 30 NOV 2017
Accepted 13 FEB 2018
Accepted article online 28 FEB 2018



# Was the Deepwater Horizon Well Discharge Churn Flow? Implications on the Estimation of the Oil Discharge and Droplet Size Distribution

**Michel C. Boufadel[1], Feng Gao[1], Lin Zhao[1], Tamay Özgökmen[2], Richard Miller[3], Thomas King[4], Brian Robinson[4], Kenneth Lee[4], and Ira Leifer[5]**

[1]Center for Natural Resources, Department of Civil and Environmental Engineering, New Jersey Institute of Technology, Newark, NJ, USA, [2]Rosenstiel School of Marine and Atmospheric Science, University of Miami, Miami, FL, USA, [3]Department of Mechanical Engineering, Clemson University, Clemson, SC, USA, [4]Bedford Institute of Oceanography, Department of Fisheries and Oceans, Dartmouth, Nova Scotia, Canada, [5]Bubbleology Research International, Solvang, CA, USA

**Abstract** Improved understanding of the character of an uncontrolled pipeline flow is critical for the estimation of the oil discharge and droplet size distribution both essential for evaluating oil spill impact. Measured oil and gas properties at the wellhead of the Macondo255 and detailed numerical modeling suggested that the flow within the pipe could have been "churn," whereby oil and gas tumble violently within the pipe and is different from the bubbly flow commonly assumed for that release. The churn flow would have produced 5 times the energy loss in the pipe compared to bubbly flow, and its plume would have entrained 35% more water than that of the bubbly flow. Both findings suggest that the oil discharge in Deepwater Horizon could have been overestimated, by up to 200%. The resulting oil droplet size distribution of churn flow is likely smaller than that of bubbly flow.

## 1. Introduction

Currently, petroleum hydrocarbons are the dominant energy source of modern society (McFarland, 2017), yet its production and transport present a significant risk to the environment and society through spills and other accidental releases (National Research Council, 2003). During its journey from the geological reservoir to end users, it flows through pipelines, where the flow can be complex. For example, controlled pipeline flow can range from laminar to stratified to turbulent flow with special cases of slug and churn flows (Hewitt & Hall Taylor, 1970). Complicating the flow is its multiphase nature, with gas, oil (generally emulsified—an oil-water suspension), additives, and in production flow pipelines, hydrates of methane and other gases as well as condensates being transported. As oil production shifts into deeper waters and Arctic waters, the challenge of an effective response to a pipeline blowout increases. Key to response decisions is the character of the flow rate, which in turn informs on the flowrate magnitude and the resulting oil droplet size distribution (DSD). Therefore, improved understanding of the character of an uncontrolled pipeline flow is critical to effective response decisions.

During the Deepwater Horizon (DWH) oil spill, the U.S. Interagency and Academia Flow Rate Technical Group (FRTG) (2011) was tasked to derive the best flow estimate—an enormous responsibility. Unfortunately, mitigation strategies failed, leading to a massive oil release and the resultant damage to the ecosystem, human health, and the regional economy. Estimates of the released oil volume varied from 3.26 to 5.0 million barrels (450,000 to 700,000 tons) (McNutt et al., 2012), making it the largest accidental oil spill in modern history. Emissions also included up to 500,000 tons of gaseous hydrocarbons (Joye et al., 2011). As the only deep-sea blowout with supporting observations, we investigate the character of the uncontrolled flow of the DWH wellhead to provide guidance for application to future subsea oil releases.

In a vertical pipe with straight, smooth walls, the magnitudes of the superficial velocities (or fluxes) determine, to a large extent, the hydrodynamics of two-phase flow in vertical pipes (Hewitt et al., 1985; Jayanti et al., 1993), see Figure 1. We address irregular walled pipes in section 4. For the bubbly flow regime, the liquid is the carrier fluid and the hydrodynamics are mainly that of liquid flow. The other extreme (annular flow) requires mostly a gas well, which does not support the economics of deepwater production. Slug flow is highly distinct from bubbly flow, with laminar fluid forcing between the gas (or oil) slugs and the walls.

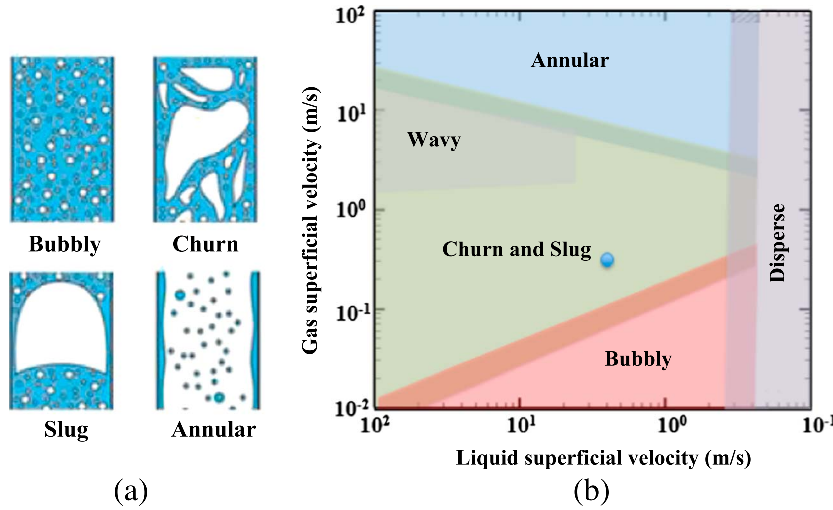


**Figure 1.** (a) Schematic of the main multiphase flow regimes in a vertical pipe. (b) Flow regime "map" adapted from Weisman (1983) including transition regimes. Wavy flow is a special case of churn/slug flow. The blue disk reflects the Deepwater Horizon condition.

Slugs are large regions (relative to the pipe diameter) where phases have separated. In slug flow, the local gas to oil ratio and flow rates vary dramatically with time. If higher gas flow rates lead to the partial breakup of slugs, turbulent churn flow results with flow reversals not only along walls but also in recirculation flows around the gas voids (Boure et al., 1973; Iguchi et al., 1992).

Formidable efforts were implemented early on to estimate the oil flow rate from the Mississippi Canyon Macondo Well (MC 252), including the formation of the FRTG. Following the explosion, hydrocarbons were released mainly from a 200 m long broken riser, lying on the sea floor, and from the kink in the riser until 3 June 2010, when the riser was cut at the wellhead, allowing direct hydrocarbon release from the cut wellhead.

Modeling of the oil flow rate within the approximately 2,000 m riser (from the reservoir to sea floor) was conducted by various groups including five U.S. Department of Energy national laboratories (Guthrie et al., 2011; McNutt et al., 2012). The rate of hydrocarbon emission from the DWH blowout was debated widely, but the ultimate release rate estimates from seabed video ranged from 62,500 to 68,000 barrels of oil per day (bopd) (FRTG, 2011), while the remote sensing-derived upper limit estimate was 84,000 bopd (Leifer et al., 2012). Uncertainty in these values was estimated at 20% for times when data were available; extrapolation to the duration of the spill increases uncertainty as flow rates were variable (Crone & Tolstoy, 2010; Leifer, 2010).

The gas to oil ratio of the cut DWH well pipe was estimated at 285 $m^3$ of gas (under standard conditions) per cubic meter of liquid oil (1,600 standard cubic feet of gas per standard barrel of oil) (Reddy et al., 2012; Zhao et al., 2017). Based on the pressure and temperature at the DWH well orifice (Text S1 in the supporting information), the volume of the solution gas (i.e., gas dissolved in oil) was ~111 $m^3$ of gas (under standard temperature and pressure) per $m^3$ of liquid oil, termed "live" oil. This is in contrast to oil without dissolved gas, termed "dead" oil (Lake & Fanchi, 2006). Thus, the separate gas phase fraction is 174 $m^3$ per $m^3$ of liquid oil. Using the oil and gas flow rates of 0.08 $m^3$/s and 0.055 $m^3$/s at the orifice of the MC252 and the riser's internal diameter of 0.5 m, one obtains a gas superficial velocity (total gas flow rate divided by the cross-section area) of ~0.3 m/s and a liquid live oil superficial velocity of ~0.4 m/s (Text S1). McNutt et al. (2011) concluded that the oil flow rate was 0.055–0.074 $m^3$/s for the post riser cut operation, equivalent to 0.3–0.4 m/s for the oil velocity. This is similar to our estimation of 0.4 m/s for live oil velocity. Our estimated live oil superficial velocity of ~0.4 m/s (equivalent to 0.08 $m^3$/s for the oil flow rate) also is comparable to the "best estimate" oil flow rate of 0.064–0.083 $m^3$/s for the post riser cut on 3 June 2010 (McNutt et al., 2011).

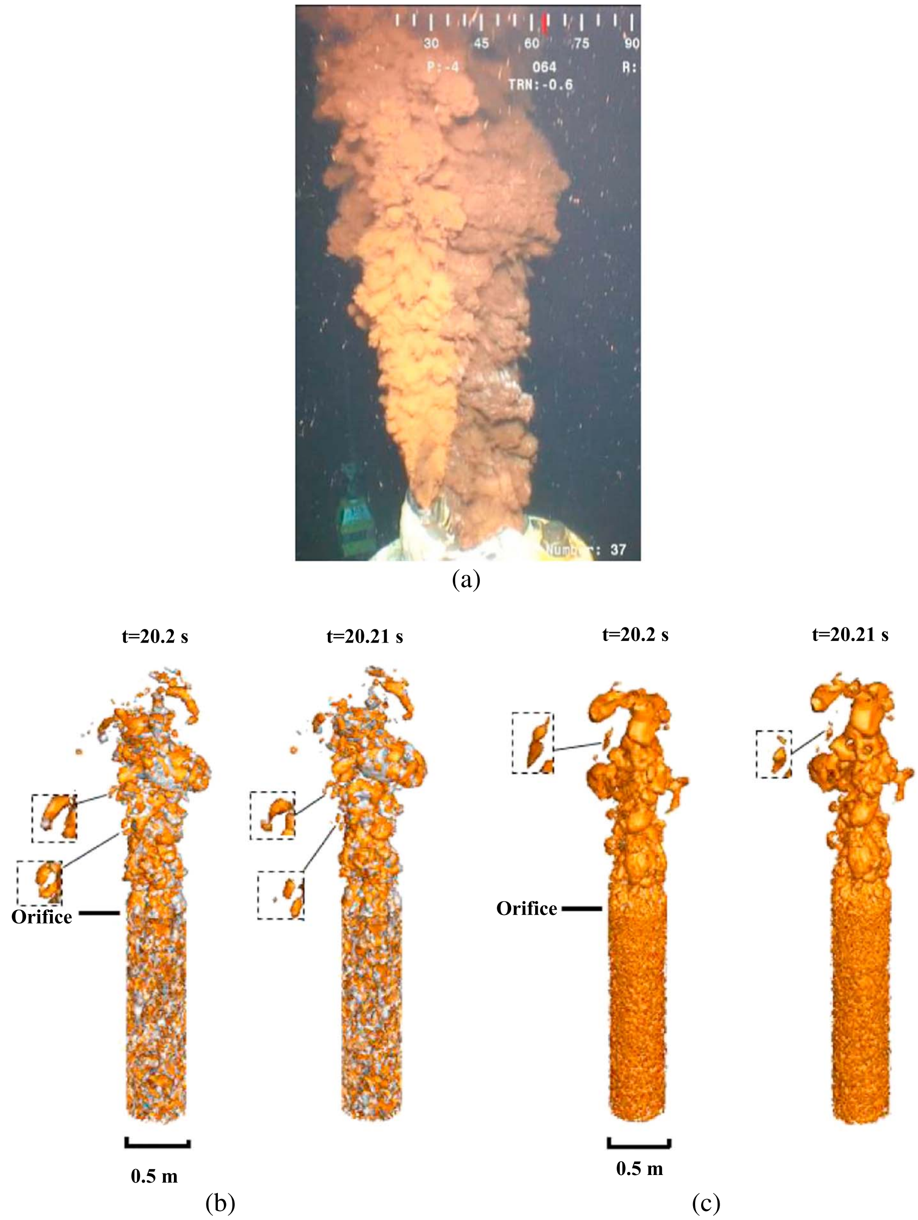


**Figure 2.** (a) Image of the Macondo252 wellhead on 3 June' 2010. (b, c) Simulated oil holdup (orange) and gas holdup (gray) at 2 times for churn flow and bubbly flow, respectively. Oil holdup threshold = 0.2, gas holdup threshold = 0.04. The simulated churn flow plume (Figure 2b) appeared "grainy," similar to photos of the actual plume (Figure 2a). The bubbly plume (Figure 2c) appears smoother. Photo from video courtesy of Lisa Di Pinto, NOAA Natural Resources Damage Assessment.

Based on these velocities and presuming a smooth pipe flow, DWH flow is "churn" (Figure 1) whose hydrodynamics is very different from that of bubbly flow, assumed to have occurred in the riser of the DWH (McNutt et al., 2011; Plume Calculation Team, 2010). Note, a threefold to fourfold reduction in the gas flow rate would be required to shift the behavior from churn flow (to bubbly flow). Of course, there is the potential for such reductions from obstructions in the riser pipe; however, as no data on the presence of irregularities are available, we address this possibility in section 4.

Here we support the qualitative inference from Figure 1 with detailed computational fluid dynamics simulations of oil and gas in a 16 m portion (Figure S1) along the flow including the riser's last 4 m and through 12 m above the riser into the deep sea to investigate the blowout's near-field flow.

## 2. Methods

We used large eddy simulation (LES) within the model FLUENT (http://www.ansys.com) to simulate the three-phase system: oil, gas, and water using the volume of fluid module (Text S2) (ANSYS, 2009; Chumakov, 2005; Hirt & Nichols, 1981; Houghtalen et al., 2016; Kraichnan, 1970; Sagaut, 2005; Stefano et al., 2008; Zhao et al., 2014). The domain consisted of ~$14.5 \times 10^6$ computational nodes and the time step was 0.2 ms to resolve turbulence scales as much as possible. Fluids were assumed incompressible within the domain. The simulation incorporated the impact of the interfacial tension between water, oil, and gas (Text S2) (Brackbill et al., 1992; Francois & Sicilian, 2007; Smirnov et al., 2001). For comparison, a simulation was conducted for bubbly pipe flow with an input oil velocity of 0.7 m/s and a 5% gas fraction. The larger initial velocity (0.7 m/s in comparison to 0.4 m/s) was intended to compensate for buoyancy loss from the small gas fraction in the bubbly flow (5% versus 45% for churn flow). The bubbly flow results are normalized by the average oil velocity to negate effects from the increase in oil velocity on the bubbly flow hydrodynamics. The simulation findings have implications with respect to droplet sizes and thus dispersant application efficacy; however, the oil DSD is beyond this study's scope.

## 3. Results

Photos of the Macondo wellhead show a highly turbulent flow escaping from the cut wellpipe in Figure 2a, with fluids emanating from it. The oil holdup (volume of oil per total volume of a given cell) and gas holdup (volume of gas per total volume of a given cell) obtained from the simulations of churn flow and bubbly flow are reported at two times. More information on the velocity within the churn flow pipe is reported in Figure S2. The simulations show downwelling flow at the walls (Figures 2, S2a, and S2b), consistent with prior observations of churn flow (Laborde-Boutet et al., 2009; Montoya et al., 2016; Parsi et al., 2015). One implication of churn flow is increased granularity in the holdup distribution compared to bubbly flow (Figure 2b versus Figure 2c), and thus resembling far more closely the DWH plume appearance (Figure 2a). Vertical and horizontal cuts through the modeled pipe and plume (Figures S3 and S4) further elucidate the unsteadiness of churn flow hydrodynamics.

Both the normalized oil and gas holdups of churn flow decreased slower as a function of the radius of the plume in comparison with those of bubbly flow (Figure 3, see Figure S5 for nonnormalized values). Of particular interest is the large gas holdup at the plume's edge ($r$ = 0.5 m) (Figures 3 and S5), which would have dispersant application implications. Additionally, the centerline oil holdup of churn flow decreased faster as a function of elevation than that of bubbly flow (Figure S6). This indicates that churn flow drives larger water entrainment from the surrounding water.

Figure S7 reports the normalized total energy dissipation rate $\frac{\varepsilon D}{U^3}$ for churn flow and bubbly flow at height, $z$ = 1.0 m (i.e., within the pipe) and $z$ = 3.0 m. At $z$ = 1.0 m, the churn flow value was 5 times larger than that of bubbly flow. The large energy loss results from the violent interaction between the phases, an interaction relied upon for cooling nuclear reactors (Bestion, 2010). For churn flow at $z$ = 3.0 m, $\frac{\varepsilon D}{U^3}$ increased only slightly in comparison with that at $z$ = 1.0 m. However, for bubbly flow, the value of $\frac{\varepsilon D}{U^3}$ more than doubled at $z$ = 3.0 m in comparison to $z$ = 1.0 m, which is consistent with the literature (Griffiths, 2012). Thus, at $z$ = 3.0 m, the normalized total energy dissipation rate for churn flow was around 2.5 times that of bubbly flow, which is consistent with the ratio of 2.0 of maximum streamwise turbulence intensities between churn flow and bubbly flow (Figure S8) (Iqbal & Thomas, 2007; Poole & Hall, 2014; Rahai & Wong, 2002; Shim et al., 2013).

The velocity profiles of the plume outside the riser obtained by temporally averaging (over 4 s) and radially averaging the axial velocity of the bubbly and churn flow are reported in Figure S10, which also shows the Gaussian distribution fit based on the equation $W(r,z)/W(0,z) = \exp\left(-\frac{a^2}{(z-2)^2}r^2\right)$, where $z$ is the elevation. Using Excel to fit the Gaussian distribution to the bubbly flow and churn flow gave $a^2$ values of 55 and 30 at $z$ = 4.0 m. The small value of churn flow reflects a gentler decrease of the churn flow velocity with the radial distance (i.e., the profile is flatter). At $z$ = 4.0 m and $r$ = 0.50 m, the churn flow velocity value was 20% the maximum, almost double that of the bubbly flow value at the same location, which is likely due to the large gas holdup at ($z$ = 4.0 m; $r$ = 0.5 m) for churn flow (Figure 3) causing large buoyancy. Thus, the churn flow plume interacts more with the surrounding water body than that of a bubbly plume.

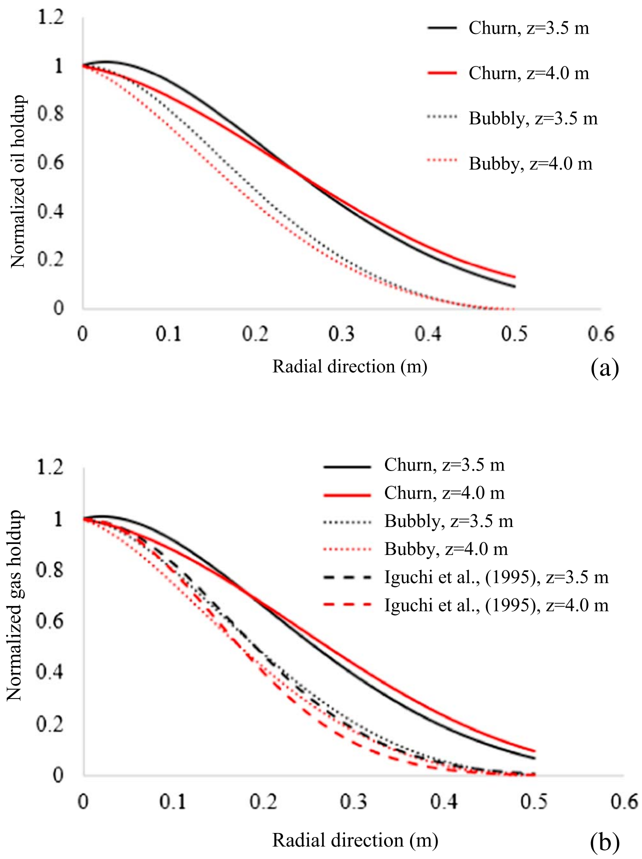


**Figure 3.** Behavior of oil and gas in the blowout (i.e., above the Deepwater Horizon riser) at two elevations, $z$, above the orifice located at $z = 2.0$ m. The normalized holdup of (a) oil and (b) gas for the churn and bubbly flows based on the large eddy simulation. The decrease as a function of the radius is slower for churn flow. Also shown are experimental bubbly flow data from Iguchi et al. (1995), with good model agreement.

An important parameter for characterizing plume behavior is the entrainment coefficient, $\alpha_E$, which represents the ratio of the entrained water volume to the total fluid volume in the plume, and has been the topic of numerous investigations (Carazzo et al., 2006; Chen & Rodi, 1980; Fischer et al., 1979). By integrating the instantaneous velocities between $z = 3.0$ m and $z = 3.1$ m (Text S4 and Figure S11 in the supporting information), we found $\alpha_E$ to be 0.15–0.16 for churn flow and 0.11–0.12 for bubbly flow (Figure S12). Thus, the churn flow plume entrains ~35% more water than the bubbly flow plume. The larger water entrainment is consistent with the rapid reduction of the oil holdup (Figure S5) and the large velocity at the churn flow plume's edge (Figure S10).

## 4. Discussion

This is the first investigation of a blowout from a multiphase churn flow (oil and gas in water), and there were no data in the literature for comparison. The sole exception is Iguchi et al. (1995) who reported only limited data of jets of churn flow of air and water in water. The LES simulation bubbly flow results agreed closely with literature data for various properties of the plume (Figures 3b, S8, S10, and S12). This indicates that the LES robustly and accurately characterizes the general plume dynamics for both bubbly flow and as applied for churn flow.

Various groups estimated the oil discharge from the MC252 well, including the U.S. Government that formed the FRTG, which included five Department of Energy labs and various academicians (McNutt et al., 2012). With the exception of Dr. Leifer of the FRTG, all assumed bubbly flow. Dr. Leifer considered intermittent behavior in the fallen (horizontal) riser prior to 3 June 2010 and reported "slug" flow behavior with a period of tens of seconds. However, the video of the release after the riser was cut on 3 June 2010 (Movie S1) suggests a behavior closer to churn. In essence, where slug flow exhibits a short period, it becomes churn (Montoya et al., 2013).

Based on energy loss considerations, neglecting the churn flow behavior could underestimate the energy loss in the pipe by fivefolds (Figure S7), which would overestimate the oil discharge by more than 200% (actually $\sqrt{5}$).

Using fluid measurements outside of the DWH pipe, researchers (page 164 of Plume Calculation Team, 2010), estimated the discharge from the DWH based on visual observation of the external eddies within one diameter of the release based on a single-phase (or bubbly) velocity profile (Wygnanski & Fiedler, 1969). In their approach, the speed of eddies on the outer edge of the plume was assumed to be 1/1.6 to 1/2.5 the plume's centerline speed. The deviation from the single-phase (or bubbly) profile, as noted herein, would introduce uncertainty in that approach; on the one hand, the actual speed of the outer eddies could be larger, consistent with the large velocity values of churn flow at, for example, $r = 0.5$ m; $z = 4.0$ m, in comparison with the common Gaussian profile (Figure S10). This would result in a smaller estimated oil flow rate. On the other hand, the zone of high velocity near the center for churn flow is broad, resulting in a larger oil flow rate if the ratio of eddy speed to centerline speed is consistent with the assumption of the Plume Calculation Team (2010). Another group (Camilli et al., 2012) estimated oil discharge using Acoustic Doppler Current Profiler (ADCP) velocimetry, which provided the total fluid velocity, although no corrections were reported for erroneous velocities – a common feature in ADCP data of mixed phase flows (Leifer et al., 2015; Nauw et al., 2015). To account for water in the discharge flow, Camilli et al. (2012) used an entrainment coefficient of 0.056, 3 times smaller than that for churn flow (0.17 in Figure S12) and even smaller than the one for bubbly flow. Smaller entrainment coefficients would induce an overestimate in the oil discharge.

Numerous papers on the oil DSD and gas bubble size distribution have been published, for example, Gros et al. (2017), Zhao et al. (2017), and publications therein, yet they all ignored churn flow dynamics. Based on the findings herein, the droplets formed by a churn flow plume are likely to be smaller than those formed by oil only or bubbly flow plumes (all parameters being equal), because the formation of oil droplets occur through a two-breakup mechanisms: First, shear and interfacial instability on the outer surface of the jet produce ligaments in a process known as primary breakup (Gorokhovski & Herrmann, 2008). Second, these ligaments are entrained into the jet and subsequently break into droplets based both on the mixing energy (energy dissipation rate, $\varepsilon$) and the oil within the plume. This is known as secondary breakup (Zhao et al., 2016). A large $\varepsilon$ value alone cannot produce small droplets without the presence of water or gas to surround them, and thus, the holdup plays an important role in droplet formation within the first few diameters of the orifice. We saw also that churn flow spreads the gas across the plume, and thus concentrates the oil in the center (Figure 3) in comparison with the bubbly flow, which concentrates the gas (but not the liquid) in the plume center (Lima Neto et al., 2008; Milgram, 1983). Thus, churn flow is more likely to produce smaller oil droplets due to the contribution of individual bubbles to the local turbulence energy (Fabregat Tomàs et al., 2016; Zhao et al., 2016). If the dispersant is applied on the plume edge, the presence of higher gas holdup would scavenge dispersant, decreasing effectiveness.

Although the calculation was for a smooth pipe, nonuniformity including protrusions in the DWH pipe were documented and are likely to exist in future blowouts. Protrusions could be in the shape of fragments of metal from the pipe and other infrastructure and spikes that would disrupt large-scale eddies minimizing, therefore, churn flow behavior, or they could be bulky such as fragments of the drill, blocking portions of the pipe, magnifying churn flow by increasing the superficial velocities of both gas and oil. In the latter case, Figure 1 shows that the flow would remain churn if the new area remains larger than 10% of the smooth pipe area. Additionally, gashes in the pipe below the seabed were likely with some of the blowout flowing outside the riser for some of its path. Depending on the details, this could make churn flow more or less likely. Given the significant implications of whether the flow is churn or bubbly, it is critical to consider, in any efforts to assess future blowouts, to evaluate both types of flow and ideally to collect data to confirm one or the other.

In future deep-sea oil and gas spills, correctly assessing the character of the flow in the pipe is critical to providing more reliable estimates for the response. Churn/slug flow has been well studied in conduits, and this study highlights the need to incorporate knowledge in analyzing geophysical multiphase flows. Still, additional complexity must be considered in future studies to reflect the complexity of reality, including pipe shape, hydrates, condensates, produced water, and the many additives used in production activities. Furthermore, such studies can identify key measurements needed to confirm flow character, decreasing uncertainty. Although the precise details of the conditions of the interior of the pipe are unlikely to be known for a blowout, studies to characterize the flow for a range of conditions would provide more robust uncertainty on estimated flow rates. Any response decisions must address both the best estimated flow rate plus 1 or 2 $\sigma$ deviation due to uncertainty to ensure success.

**Acknowledgments**
This research was made possible by a grant from the Gulf of Mexico Research Initiative through the Consortium CARTHE II, and by the Department of Fisheries and Ocean Canada (DFO). Data are publicly available through the Gulf of Mexico Research Initiative Information and Data Cooperative (GRIIDC) at https://data.gulfresearchinitiative.org (doi: 10.7266/N7Q23XS7). However, it does not reflect the views of these entities, and no official endorsement should be implied. We would like to thank Lisa Di Pinto for the courtesy of providing the video of the oil release after the riser was cut on 3 June 2010. The authors declare no conflict of interest.

## References

ANSYS (2009). *Fluent 12.0 user's guide*. Canonsburg, PA: ANSYS, Inc.

Bestion, D. (2010). From the direct numerical simulation to system codes—Perspective for the multi-scale analysis of LWR thermal hydraulics. *Nuclear Engineering and Technology*, *42*(6), 608–619. https://doi.org/10.5516/NET.2010.42.6.608

Boure, J. A., Bergles, A. E., & Tong, L. S. (1973). Review of two-phase flow instability. *Nuclear Engineering and Design*, *25*(2), 165–192. https://doi.org/10.1016/0029-5493(73)90043-5

Brackbill, J. U., Kothe, D. B., & Zemach, C. (1992). A continuum method for modeling surface tension. *Journal of Computational Physics*, *100*(2), 335–354. https://doi.org/10.1016/0021-9991(92)90240-Y

Camilli, R., Di Iorio, D., Bowen, A., Reddy, C. M., Techet, A. H., Yoerger, D. R., et al. (2012). Acoustic measurement of the Deepwater Horizon Macondo well flow rate. *Proceedings of the National Academy of Sciences of the United States of America*, *109*(50), 20,235–20,239. https://doi.org/10.1073/pnas.1100385108

Carazzo, G., Kaminski, E., & Tait, S. (2006). The route to self-similarity in turbulent jets and plumes. *Journal of Fluid Mechanics*, *547*, 137–148. https://doi.org/10.1017/S002211200500683X

Chen, C. J., & Rodi, W. (1980). Vertical turbulent buoyant jets: A review of experimental data. *Annual Review of Heat Transfer*, *4*, 94.

Chumakov, S. (2005). *Subgrid models for large eddy simulation: Scaler flux, scaler dissipation and energy dissipation*, (PhD). University of Wisconsin-Madison.

Crone, T. J., & Tolstoy, M. (2010). Magnitude of the 2010 Gulf of Mexico oil leak. *Science*, *330*(6004), 634–634. https://doi.org/10.1126/science.1195840

Fabregat Tomàs, A., Poje, A. C., Özgökmen, T. M., & Dewar, W. K. (2016). Dynamics of multiphase turbulent plumes with hybrid buoyancy sources in stratified environments. *Physics of Fluids*, *28*(9), 095109. https://doi.org/10.1063/1.4963313

Fischer, J. E. L., Koh, C. R., Imberger, J., & Brooks, N. H. (1979). *Mixing in inland and coastal waters* (p. iv). San Diego: Academic Press.
Flow Rate Technical Group (FRTG) (2011). *Assessment of flow rate estimates for the Deepwater Horizon/Macondo well oil spill*. Washington, DC: U.S. Department of the Interior.
Francois, M., & Sicilian, J. (2007). *Modeling interfacial surface tension in fluid flow*. Oak Ridge, TN: Oak Ridge National Laboratory.
Gorokhovski, M., & Herrmann, M. (2008). Modeling primary atomization. *Annual Review of Fluid Mechanics*, *40*(1), 343–366. https://doi.org/10.1146/annurev.fluid.40.111406.102200
Griffiths, S. K. (2012). Oil release from Macondo well MC252 following the Deepwater Horizon accident. *Environmental Science & Technology*, *46*(10), 5616–5622. https://doi.org/10.1021/es204569t
Gros, J., Socolofsky, S. A., Dissanayake, A. L., Zhao, L., Boufadel, M. C., Reddy, C. M., & Arey, J. S. (2017). Petroleum dynamics in the sea and influence of subsea dispersant injection during Deepwater Horizon. *Proceedings of the National Academy of Sciences of the United States of America*, *114*, 10,065–10,070.
Guthrie, G., Pawar, R., Oldenburg, C., Weisgraber, T., Bromhal, G., & Gauglitz, P. (2011). *Nodal analysis estimates of fluid flow from the BP Macondo MC252 well*. Washington, DC: U.S. Department of the Interior.
Hewitt, G., & Hall Taylor, N. (1970). *Annular two-phase flow*. Oxford: Pergamon Press.
Hewitt, G. F., Martin, C. J., & Wilkes, N. S. (1985). Experimental and modelling studies of annular flow in the region between flow reversal and the pressure drop minimum. *Physicochemical Hydrodynamics*, *6*, 69–86.
Hirt, C. W., & Nichols, B. D. (1981). Volume of fluid (VOF) method for the dynamics of free boundaries. *Journal of Computational Physics*, *39*(1), 201–225. https://doi.org/10.1016/0021-9991(81)90145-5
Houghtalen, R. J., Osman, A., & Hwang, N. H. (2016). *Fundamentals of hydraulic engineering systems*. New York: Prentice Hall.
Iguchi, M., Ueda, H., & Uemura, T. (1995). Bubble and liquid flow characteristics in a vertical bubbling jet. *International Journal of Multiphase Flow*, *21*(5), 861–873. https://doi.org/10.1016/0301-9322(95)00014-O
Iguchi, M., Uemura, T., Yamamoto, F., & Morita, Z. (1992). Multiphase flows in ironmaking and steel-making processes. *Japanese Journal of Multiphase Flow*, *6*(1), 54–64. https://doi.org/10.3811/jjmf.6.54
Iqbal, M. O., & Thomas, F. O. (2007). Coherent structure in a turbulent jet via a vector implementation of the proper orthogonal decomposition. *Journal of Fluid Mechanics*, *571*, 281–326. https://doi.org/10.1017/S0022112006003351
Jayanti, S., Hewitt, G. F., Low, D. E. F., & Hervieu, E. (1993). Observation of flooding in the Taylor bubble of co-current upwards slug flow. *International Journal of Multiphase Flow*, *19*(3), 531–534. https://doi.org/10.1016/0301-9322(93)90066-4
Joye, S. B., MacDonald, I. R., Leifer, I., & Asper, V. (2011). Magnitude and oxidation potential of hydrocarbon gases released from the BP oil well blowout. *Nature Geoscience*, *4*(3), 160–164. https://doi.org/10.1038/ngeo1067
Kraichnan, R. H. (1970). Diffusion by a random velocity field. *Physics of Fluids*, *13*(1), 22–31. https://doi.org/10.1063/1.1692799
Laborde-Boutet, C., Larachi, F., Dromard, N., Delsart, O., & Schweich, D. (2009). CFD simulation of bubble column flows: Investigations on turbulence models in RANS approach. *Chemical Engineering Science*, *64*(21), 4399–4413. https://doi.org/10.1016/j.ces.2009.07.009
Lake, L. W., & Fanchi, J. R. (2006). *Petroleum engineering handbook: General engineering*. Richardson, TX: Society Of Petroleum Engineers.
Leifer, I. (2010). Characteristics and scaling of bubble plumes from marine hydrocarbon seepage in the Coal Oil Point seep field. *Journal of Geophysical Research*, *115*, C11014. https://doi.org/10.1029/2009JC005844
Leifer, I., Lehr, W. J., Simecek-Beatty, D., Bradley, E., Clark, R., Dennison, P., et al. (2012). State of the art satellite and airborne marine oil spill remote sensing: Application to the BP Deepwater Horizon oil spill. *Remote Sensing of Environment*, *124*, 185–209. https://doi.org/10.1016/j.rse.2012.03.024
Leifer, I., Solomon, E., Schneider, V., Deimling, J., Coffin, R., Rehder, G., & Linke, P. (2015). The fate of bubbles in a large, intense bubble plume for stratified and unstratified water: Numerical simulations of 22/4b expedition field data. *Journal of Marine and Petroleum Geology*, *68B*, 806–823.
Lima Neto, I. E., Zhu, D. Z., & Rajaratnam, N. (2008). Bubbly jets in stagnant water. *International Journal of Multiphase Flow*, *34*(12), 1130–1141. https://doi.org/10.1016/j.ijmultiphaseflow.2008.06.005
McFarland, A. (2017). Total U.S. energy production falls in 2016 after six consecutive years of increases. Washington, DC: U.S. Energy Information Administration.
McNutt, M. K., Camilli, R., Crone, T. J., Guthrie, G. D., Hsieh, P. A., Ryerson, T. B., et al. (2012). Review of flow rate estimates of the Deepwater Horizon oil spill. *Proceedings of the National Academy of Sciences of the United States of America*, *109*(50), 20,260–20,267. https://doi.org/10.1073/pnas.1112139108
McNutt, M., Camilli, R., Guthrie, G., Hsieh, P., Labson, V., Lehr, B., et al. (2011). Assessment of flow rate estimates for the Deepwater Horizon/Macondo well oil spill, Flow Rate Technical Group report to the National Incident Command, Interagency Solutions Group, March 10, 2011.
Milgram, J. H. (1983). Mean flow in round bubble plumes. *Journal of Fluid Mechanics*, *133*, 345–376. https://doi.org/10.1017/S0022112083001950
Montoya, G., Liao, Y., Lucas, D., & Krepper, E. (2013). Analysis and applications of a two-fluid multi-field hydrodynamic model for churn-turbulent flows. In *Proceedings 2013 21st International Conference on Nuclear Engineering*, *American Society of Mechanical Engineers* (pp. V006T16A033–V006T16A046). Chengdu, China.
Montoya, G., Lucas, D., Baglietto, E., & Liao, Y. (2016). A review on mechanisms and models for the churn-turbulent flow regime. *Chemical Engineering Science*, *141*, 86–103. https://doi.org/10.1016/j.ces.2015.09.011
National Research Council (2003). *Oil in the Sea III: Inputs, fates, and effects* (p. 265). Washington, DC: National Academy of Sciences.
Nauw, J., Linke, P., & Leifer, I. (2015). Bubble momentum plume as a possible mechanism for an early breakdown of the seasonal stratification in the northern North Sea. *Journal of Marine and Petroleum Geology*, *68*, 789–805. https://doi.org/10.1016/j.marpetgeo.2015.05.003
Parsi, M., Vieira, R. E., Torres, C. F., Kesana, N. R., McLaury, B. S., Shirazi, S. A., et al. (2015). Experimental investigation of interfacial structures within churn flow using a dual wire-mesh sensor. *International Journal of Multiphase Flow*, *73*, 155–170. https://doi.org/10.1016/j.ijmultiphaseflow.2015.03.019
Plume Calculation Team (2010). *Deepwater Horizon release estimate of rate by PIV*. Washington, DC: U.S. Department of the Interior.
Poole, B., & Hall, J. W. (2014). Turbulence measurements in the corner wall jet. In *Proceedings of the ASME 2014 International Mechanical Engineering Congress and Exposition* (pp. V007T09A092).
Rahai, H. R., & Wong, T. W. (2002). Velocity field characteristics of turbulent jets from round tubes with coil inserts. *Applied Thermal Engineering*, *22*(9), 1037–1045. https://doi.org/10.1016/S1359-4311(02)00016-9
Reddy, C. M., Arey, J. S., Seewald, J. S., Sylva, S. P., Lemkau, K. L., Nelson, R. K., et al. (2012). Composition and fate of gas and oil released to the water column during the Deepwater Horizon oil spill. *Proceedings of the National Academy of Sciences of the United States of America*, *109*(50), 20,229–20,234. https://doi.org/10.1073/pnas.1101242108

Sagaut, P. (2005). *Large eddy simulation for incompressible flows*. Berlin, Germany: Springer.
Shim, Y. M., Sharma, R. N., & Richards, P. J. (2013). Proper orthogonal decomposition analysis of the flow field in a plane jet. *Experimental Thermal and Fluid Science*, *51*, 37–55. https://doi.org/10.1016/j.expthermflusci.2013.06.014
Smirnov, A., Shi, S., & Celik, I. (2001). Random flow generation technique for large eddy simulations and particle-dynamics modeling. *Journal of Fluids Engineering*, *123*(2), 359–371. https://doi.org/10.1115/1.1369598
Stefano, G. D., Vasilyev, O. V., & Goldstein, D. E. (2008). Localized dynamic kinetic-energy-based models for stochastic coherent adaptive large eddy simulation. *Physics of Fluids*, *20*(4), 045102. https://doi.org/10.1063/1.2896283
Weisman, J. (1983). *Two-phase flow patterns, Handbook of fluids in motion* (pp. 409–425). Ann Arbor, MI: Ann Arbor Science.
Wygnanski, I., & Fiedler, H. E. (1969). Some measurements in the self-preserving jet. *Journal of Fluid Mechanics*, *38*(03), 577–612. https://doi.org/10.1017/S0022112069000358
Zhao, L., Boufadel, M. C., King, T., Robinson, B., Gao, F., Socolofsky, S. A., & Lee, K. (2017). Droplet and bubble formation of combined oil and gas releases in subsea blowouts. *Marine Pollution Bulletin*, *120*(1-2), 203–216. https://doi.org/10.1016/j.marpolbul.2017.05.010
Zhao, L., Boufadel, M. C., Socolofsky, S. A., Adams, E., King, T., & Lee, K. (2014). Evolution of droplets in subsea oil and gas blowouts: Development and validation of the numerical model VDROP-J. *Marine Pollution Bulletin*, *83*(1), 58–69. https://doi.org/10.1016/j.marpolbul.2014.04.020
Zhao, L., Shaffer, F., Robinson, B., King, T., D'Ambrose, C., Pan, Z., et al. (2016). Underwater oil jet: Hydrodynamics and droplet size distribution. *Chemical Engineering Journal*, *299*, 292–303. https://doi.org/10.1016/j.cej.2016.04.061